Published in final edited form as:

Stroke. 2008 June ; 39(6): 1862–1868. doi:10.1161/STROKEAHA.107.506352.

Early Diffusion-Weighted MRI as a Predictor of Caspase-3 Activation After Hypoxic–Ischemic Insult in Neonatal Rodents

Michael F. Wendland, PhD, **Joel Faustino, BS**, **Tim West, PhD**, **Catherine Manabat, BS**, **David M. Holtzman, MD**, and **Zinaida S. Vexler, PhD**

Departments of Radiology (M.F.W.) and Neurology (J.F., C.M., Z.S.V.), University of California–San Francisco, San Francisco, Calif; and the Departments of Neurology, Molecular Biology & Pharmacology and the Hope Center for Neurological Disorders (T.W., D.M.H.), Washington University School of Medicine, St Louis, Mo

Abstract

Background and Purpose—Neonatal encephalopathy in human babies is a serious condition associated with permanent neurological deficits. Diffusion-weighted MRI (DWI) is increasingly used for early diagnosis of brain injury in human babies. The relationship between the presence of DWI abnormalities and cellular injury, including apoptosis, during the neonatal period are not well understood. We asked whether the extent of injury depicted on DWI can predict the presence of caspase-3 activation, a quantitative marker of apoptotic injury, after hypoxia–ischemia (H-I) in postnatal day 7 rats.

Methods—Injury volume was determined by DWI at 2 hours, 24 hours, and 7 days after H-I and compared with histology. Caspase-3 activation and microgliosis were determined at 24 hours post-H-I.

Results—DWI-defined lesions (eg, decreased apparent diffusion coefficient) at 24 hours post-H-I correlated with a major increase in caspase-3 activity in the injured hemisphere and predicted injury. A modest but significant increase in caspase-3 activity occurred in the cortex of rats that had no apparent diffusion coefficient decrease in the injured hemisphere but had unilaterally enlarged regions of high apparent diffusion coefficient at the ipsilateral ventricle/white matter interface. Caspase-3 activity was similar in both hemispheres in pups with unchanged DWI.

Conclusions—Abnormal DWI signal at 24 hours post-H-I is predictive of caspase-3 activation and can be used as an indicator that injury involving an apoptotic-like mechanism is present. Our data also suggest that the presence of an enlarged unilateral region with high apparent diffusion coefficient at the ventricle/white matter interface without significant apparent diffusion coefficient decrease in the cortex is a sign of modest caspase-3 activation after H-I.

Correspondence to Zinaida S. Vexler, PhD, University California–San Francisco, Department of Neurology, Box 0663, 521 Parnassus Ave, San Francisco, CA 94143-0663. Zena.Vexler@ucsf.edu.

Disclosures

None.

Keywords

apoptosis; caspase-3; diffusion-weighted MRI; hypoxia–ischemia; neonate

Serial noninvasive neuroimaging, MRI and spectroscopy, in both humans and in animal models, have shown that injury patterns depend on the severity of the insult and the age at which it occurs[1] and that brain injury evolves over days and even weeks.[2] The diagnostic capabilities of MRI have been used in adult stroke models for a long time, but its use in neonatal animal models has been scarce. Diffusion-weighted MRI (DWI) performed in naïve animals of different ages and the apparent diffusion coefficient (ADC) derived from DWI showed that water diffusion is substantially less restricted in the neonatal compared with the adult brain, consistent with the lack of brain myelination. Furthermore, the extent of ADC reduction after focal stroke or hypoxia–ischemia (H-I) is substantially larger in neonates[3–7] than in adults.[8] We and others have shown that the decrease in ADC is biphasic in the neonatal brain after focal stroke or H-I,[9–11] that the first drop occurs much earlier than cell death, and that secondary decline of the ADC is associated with structural injury.[9–11] Although redistribution between extracellular and intracellular water plays a major role,[12,13] the extent of associated metabolic stress and altered intracellular molecular interactions is not fully understood.

Compared with the adult brain after stroke or trauma, neonatal brain is much more susceptible to activation of apoptotic pathways[14,15] likely due to ongoing developmental elimination of neurons by apoptosis at this stage in development. Apoptosis in the neonatal brain correlates highly with activation of the executioner caspase, caspase-3, enabling the use of caspase-3 activation as a measure of long-term injury outcome after neonatal H-I.[16] Identification of a noninvasive surrogate indicator for caspase-3 activation during early injury stages, in turn, may prove to be a very useful tool in long-term studies on neuroprotection.

We asked if the extent of changes depicted on DWI can predict acute caspase-3 activation and long-term injury outcome after H-I in neonatal rats. We report here that the presence of significant ADC reduction at 24 hours post-H-I is always associated with marked caspase-3 activation and that the presence of unilaterally enlarged regions with high ADC values at the ventricular/white matter interface in the absence of ADC drop in the tissue is associated with a modest but significant caspase-3 activation.

Methods

Animal Care and Surgical Procedure

All animal research was approved by the University of California–San Francisco Institutional Animal Care and Use Committee and was performed in accordance with the Guide for the Care and Use of Laboratory Animals (US Department of Health and Human Services, Publication Number 85–23, 1985). Female Sprague-Dawley rats with a 6-day-old litter were housed in a temperature-/light-controlled environment and given food and water

ad libitum. Postnatal day 7 rats were exposed to right common carotid artery ligation followed by hypoxia (8% O_2/N_2) for 2.5 hours, H-I, as previously described.[14]

MRI

Pups were imaged 3 times at 2 hours, 24 hours, and 7 days after H-I for injury volume measurements or either at 2 to 3 hours after H-I for measurements of caspase-3-dependent and -independent spectrin cleavage at 5 hours or at 24 hours after H-I for measurements of caspase-3 activity at the end of the imaging session. Images were acquired in anesthetized rats using a Bruker 2T system as described.[10] Multislice T2 and DWI (b factor= 1030 seconds/mm^2 applied along the Z-axis) spin echo images were acquired with TR/TE=2500/60ms, field of view=32 mm, matrix=128×128 (in-plane pixel dimension of 0.25 mm), and 8 contiguous slices, 1 mm thick, 4 signal averages, 1-hour acquisition time. Signal-to-noise ratio for brain tissue was 28 to 40 on T2-weighted images. Images were analyzed using commercially available software (MRvision; The MRVision Co., Winchester, Mass). ADC maps were calculated from T2-weighted and DWI for each animal using the equation ADC=−ln[SI(DW)/SI(T2)]/b, where SI is pixel signal intensity of the indicated image.[10] On the ADC map, the size of apparent injury was determined by counting the number of pixels in the hemisphere ipsilateral to common carotid artery ligation with a threshold signal intensity < mean −2 SD of contralateral hemisphere in each slice normalized to total ipsilateral brain pixels. The size of the ventricular space/white matter interface was quantified on ADC maps by summing all pixels with ADC >1.6×10^{-3} mm^2/s (eg, characteristic of simple fluid) in association with the right and left lateral ventricle regions and expressed as fraction of ipsilateral/contralateral pixels. In control animals, this ratio was 0.9±0.19 (n=5). Ventricle was considered enlarged when the ratio was larger than 1.6 and the raw difference in pixel count >30.

Caspase-3 Enzymatic Assay and Western Blotting

Tissue lysates were prepared from ipsilateral and contralateral hemispheres obtained between anterior and posterior corpus callosum, excluding cingulate. Spectrin cleavage mediated by calpain and caspase-3 was determined by Western using mouse antirat spectrin antibody (1:1000) as described.[17] Caspase-3 activity was measured as DEVD cleavage activity using Acetyl-AMC (Calbiochem, San Diego, Calif) to obtain a standard curve as described.[17] The DEVD cleavage activity was calculated as pmol/min/mg of total protein.

Histological Analysis

Brain volume was determined 7 days after H-I in paraffin-embedded coronal sections (20 μm thick cut at 400-μm intervals) obtained from paraformaldehyde perfusion-fixed animals that underwent multiple MRI sessions. Volumetric measurements were obtained from 8 cresyl violet-stained sections using Neurolucida (Microbrightfield Software Systems) as previously reported.[18] Data are expressed as a ratio of the ipsilateral tissue volume to the volume of the contralateral tissue.

Immunofluorescence

Sections were deparaffinized and immunostained as described.[19] Rabbit antirat cleaved caspase-3 (Cell Signaling; 1:150), rabbit antirat Iba-1 (Wako; 1:200), mouse antirat glial fibrillary acidic protein (Serotec; 1:50) antibodies, and secondary antibodies raised in the appropriate target species and conjugated to Cy2 or Cy3 dyes (1:100) were used. Slides were incubated in bis-benzamide (0.001%). Slides were imaged with a Zeiss Axiovert 100 florescent microscope equipped with OpenLab Software (Improvision).

Statistical Analysis

The volume of injury and ventricles and caspase-3 activity were analyzed by analysis of variance with post hoc testing (Fisher). Differences were considered significant at $P<0.05$. Results are shown as mean±SD.

Results

Progression of Diffusion-Weighted MRI-Identifiable Injury After Hypoxia–Ischemia in Postnatal Day 7 Rats

To determine whether DWI can be used as a surrogate measure of histological outcome after H-I, 10 rats were imaged at 2 hours, 24 hours, and 7 days after H-I; the volume of abnormal DWI was compared with the volume of the histological lesion after euthanasia at 7 days (Figure 1A). At 2 hours postreoxygenation, DWI lesions were evident in 2 pups (circles). By 24 hours, DWI lesions were seen in 7 animals and all 7 showed both MRI- and histologically confirmed lesions 7 days after H-I (squares). Of 3 rats with no DWI lesion at 2 or 24 hours after H-I, injury evolved in only one rat (triangles). Animals with DWI abnormalities early after H-I had overall larger lesions. In contrast, no evidence of histological lesion was observed in 2 pups with lack of DWI lesions 7 days after H-I. Calpain-mediated spectrin cleavage, which is indicative of excitotoxic injury,[17] was seen at 5 and 24 hours post-H-I in ipsilateral tissue with or without lesions on DWI 2 to 3 hours after H-I (Figure 1B). Caspase-3 -mediated spectrin cleavage was minimal at 5 hours and profound at 24 hours post-H-I. Therefore, DWI underestimates long-term injury when acquired 2 hours post-H-I, whereas it delineates the evolving injury when acquired at 24 hours post-H-I. These data also indicate that DWI changes temporally correlates with the peak in caspase-3 activation shown in our prior studies.[17]

Diffusion-Weighted MRI-Identifiable Lesions and Increase in Caspase-3 Activity 24 Hours After Hypoxia–Ischemia

A separate group of rats was imaged 24 hours post-H-I and then euthanized and assayed for caspase-3 activation. Three patterns of injury were evident by DWI (Figure 2): (1) hyperintense DWI signal and corresponding ADC drop was observed in the ipsilateral hemisphere (group 1, top); (2) normal ADC signal in the H-I cortex but an enlarged region with high ADC in the lateral ventricle in the vicinity of the white matter in the ipsilateral hemisphere (group 2, middle); and (3) unchanged ADC values in the H-I hemisphere and symmetrical appearance of regions in the vicinity to the ventricles (group 3, bottom). ADC values in the contralateral hemisphere were not different from values in control animals.

In group 1, the ADC values in the ipsilateral regions were significantly reduced ($0.60\pm0.16\times10^{-3}$ mm^2/s) compared with the contralateral cortex ($1.04\pm0.09\times10^{-3}$ mm^2/s, n=9, P=0.004). All pups in this group showed markedly increased caspase-3 activity in the ipsilateral cortex compared with contralateral regions (P=0.001; Figure 3A–B). The size and distribution of regions with abnormal ADC values varied considerably within the group, 27.6±16.8% of the ipsilateral hemisphere, with no significant correlation between caspase-3 activity and either size of injury (R^2=0.58, P=0.17) or ipsilateral ADC value (R^2=0.44, P=0.32). Calpain-mediated spectrin cleavage was seen in all animals (Figure 3C). Only modest hyperintensity was seen on T2-weighted images in the injured cortex, precluding confident delineation of injury size.

In group 2, no ADC reduction was seen in the tissue, but a 2.32±0.48-fold increase in the number of pixels with high ADC ($2.0\pm0.15\times10^{-3}$ mm^2/s, n=6) was observed at the ipsilateral lateral ventricle/white matter interface suggesting the presence of both fluid and tissue in these voxels. Pups in group 2 exhibited modest but clear and statistically significantly increased caspase-3 activity in the ipsilateral versus contralateral cortex (P=0.004; Figure 3A–B). Calpain-mediated spectrin cleavage was lower; modest caspase-3 activation produced only subtle cleavage of spectrin (Figure 3C).

In group 3, the ratio of the number of pixels with high ADC was 1.15±0.23 for ipsilateral/contralateral hemispheres in the remaining 6 pups post-H-I, not statistically different from that in the 4 control pups. Calpain-mediated spectrin cleavage (Figure 3C) and similar levels of caspase-3 activity were observed in both hemispheres (P=0.34; Figure 3B).

Distribution of Cells With Active Caspase-3 Differs After Severe and Modest Injury

The spatial pattern of caspase-3 activation was investigated using immunofluorescence. Essentially no cells with active caspase-3 were seen in the hemisphere contralateral to common carotid artery ligation (Figure 4A–C, n=3) or in either hemisphere in rats with no DWI changes (not shown). In group 2, few cells with cleaved caspase-3 were seen in the cortex (Figure 4D–I, n=3) as well as in the hippocampus and caudate (not shown). In contrast, substantial caspase-3 activation is seen in both the cortex and hippocampus of animals from group 1 (Figure 4J–O).

Modest Caspase-3 Activation Is Associated With Local Inflammation

Next we determined whether microglial activation occurs in animals from groups 1 and 2. In the contra-lateral cortex, Iba1-immunoreactive microglial cells remained quiescent based on unchanged morphology compared with controls, eg, small cell bodies and multiple long web-looking processes (Figures 5A, D, and G). Larger cell bodies and shorter processes observed within the white matter tracts in the hypoxic hemisphere (Figures 5A and E) were similar to those in naïve animals. In group 2, a range of morphologies, from quiescent cells to small patches of round cells (Figure 5H), was seen in the H-I cortex, consistent with the presence of patches of caspase-3 positive cells (Figure 4). The overall increased number of Iba1-positive cells with larger bodies and retracted processes was also seen in white matter of the H-I hemisphere. In group 1, round Iba1-positive cells were in abundance in the H-I hemisphere, spatially corresponding to injury (Figures 5C, F, I, and J). Glial fibrillary acidic

protein-immunoreactive cells were observed in the contralateral cortex, particularly around vessels, and in the white matter (Figures 5A, D, and G). In group 2, the density of glial fibrillary acidic protein-positive cells tended to increase in the H-I white matter and some reactive astrocytosis was seen in the H-I cortex in association with the presence of caspase-3 and Iba1-positive cells (Figures 5B and E). In group 1, glial fibrillary acidic protein-positive cells were seen in the periphery rather than in the center of injured cortex.

Discussion

We show that the presence of a decrease in ADC at 24 hours post-H-I is always associated with a marked increase in caspase-3 activity as detected by biochemical, functional, and immunostaining assays. We also show modest, but significantly increased, caspase-3 activation in brains without reduced ADC in the tissue but with a unilaterally enlarged region with high ADC at the ventricular white matter junction at 24 hours post-H-I. These data suggest that DWI acquired 24 hours post-H-I indicates that if DWI abnormalities are present, at a minimum, caspase-3-mediated apoptotic cell death is present.

In neonatal rodents, although pathways independent of caspase-3 are important contributors to H-I injury,[20–22] caspase-3 activation plays a central role in the pathophysiology of H-I. Caspase-3 activation starts increasing 6 to 12 hours after the injury and peaks between 24 to 36 hours after H-I.[14,15] Studies of neonatal rats and mice with perturbed apoptotic pathways have estimated that apoptosis is responsible for up to 50% of the tissue loss that occurs at 7 days after H-I,[17,23] but H-I injury varies in individual animals as shown previously by others and in this article. This raises the question of whether modest or absent injury results from a subtle acute injury or from injury resolution over time. We show that this distinction, which is important for long-term studies of neuroprotective or repair-enhancing agents, can be obtained from noninvasive estimates of caspase-3 activation during early stages of H-I.

We show that the timing of DWI acquisition plays a critical role in the ability to predict long-term injury. DWI performed shortly after reoxygenation consistently underestimates histological outcome 7 days later and fails to predict the presence of excitotoxic injury or caspase-3 activation 5 to 24 hours post H-I. In contrast, a DWI lesion in the tissue at 24 hours is associated with a major increase in caspase-3 activity at the time of imaging and translates to a histological lesion at 7 days in 9 of 10 rats. Early ischemia-induced ADC decrease is caused, in part, by redistribution of water between the extracellular and intracellular space.[13,24] The reduction in ADC in neonatal rodents during H-I is not necessarily associated with a metabolic energy failure,[3] potentially permitting apoptosis (an energy-dependent process) to occur. DWI hyperintensity is followed by renormalization of DWI signal shortly after reoxygenation as previously reported by several,[12,13,24] but not all, laboratories.[11] Our data on calpain activation at 5 hours post H-I show that excitotoxic injury in the injured hemisphere is not predicted by DWI acquired 2 to 3 hours earlier. Although limitations in DWI injury detection sensitivity may contribute to the lack of injury prediction, physiological factors associated with partial-to-complete renormalization of DWI are of importance, including variable degree of post-H-I cerebral blood flow restoration and time needed for cellular injury to substantiate.

The underlying reasons for secondary decline of the ADC recently shown after H-I or focal stroke in neonatal rodents[13,24,25] are likely to be similar to that in stroke models in adult rodents.[26] The drop of ADC parallels cerebral blood flow restoration and altered expression of a broad range of proteins, including proteins indicating the presence of metabolic stress (HSP72[26]), inflammation,[27] ongoing necrosis (calpain and clusterin[20,21]), and apoptosis (caspase-3[7,17,21]). Some reports suggest that secondary ischemia-induced energy failure is the major underlying mechanism for subsequent secondary ADC reduction,[28] whereas others show that decreased energy metabolism relates to severity and spatial distribution of initial injury.[13] Glial swelling has been suggested to contribute to the late decline of the ADC signal,[12] but glial scar formation evolves over weeks.

Apparently, secondary ADC reduction depends on multiple mechanisms that ultimately contribute to both necrosis and apoptosis, which can both be severe at 24 hours after H-I. Necrosis in the neonatal brain may be a potent trigger of apoptosis through release of toxic molecules that endanger neighboring neurons directly, by activating microglial cells and priming endothelium, and by eliminating the target of neuronal projections. In the adult, ADC reduction is most profound in the ischemic core, a region with predominant necrosis after focal ischemia–reperfusion. In contrast, in postnatal day 7 rats, an age when apoptosis and intermittent (“continuum”) cell death are most prominent,[29] caspase-3 activity is profoundly increased early after reperfusion in regions with relatively modest early reduction of the ADC, whereas a more delayed but marked caspase-3 activation is observed in the ischemic core.[7] Although caspase-3 activation is likely not the only source of ADC drop in H-I tissue, the important finding of this article is that ADC decreases 24 hours post-H-I are always associated with major caspase-3 activation. Lack of correlation between the magnitude of caspase-3 activation in animals with DWI lesions and lesion size or the extent of ADC reduction can be affected by measurements of caspase-3 activity in whole tissue homogenates obtained from regions with heterogeneous injury severity as seen both on DWI and sections immunostained for cleaved caspase-3. Partial volume error in a relatively thick DWI coronal plane can also affect correlation between 2 parameters.

Importantly, our data show that the presence of asymmetry on DWI at the ventricular/white matter interface in the absence of ADC drop within the tissue is a useful diagnostic tool for identifying cases with subtle early injury, cases with increased apoptosis without obvious necrotic lesions. The mechanisms for asymmetry are yet to be understood. The high ADC threshold used to quantify asymmetry at the lateral ventricle interface suggests an enlarged compartment of fluid. This may be due to enlarged ventricular space, tissue loss, or an intrinsic change in tissue water content in the white matter. Loss of tissue, cortical or white matter, could result in enlarged ventricle size with the consequent high ADC values, but tissue loss evolves over days, making it unlikely that tissue loss accounts for the high ADC seen at 24 hours after H-I. Another factor affecting ADC values is the partial volume error due to presence of the ventricular space and adjacent brain tissue in image voxels. In this case, reduction rather than increase of ADC in white matter would be expected acutely as seen in the cortex. Largely unchanged T2-weighted signal reduces the likelihood of vasogenic edema in the white matter. Finally, the presence of both excitotoxic component and local inflammation may affect ventricular size or fluid within the tissue in this region. Our data on gradual microglial activation both in the white matter tracts and in the cortex

may be important in interpreting DWI data. Although MRI findings consistent with increased fluid in the ventricle should correlate with increased size of the ventricles by histological analysis, histological changes were not clearly identified. However, tissue paraffin embedding and processing cause nonlinear tissue shrinkage, potentially precluding visible changes in ventricular space in the histological specimens. There have been no studies using a neonatal H-I model looking at the relationship between the effect of systemic and local inflammation and the accumulation of inflammatory mediators in the cerebrospinal fluid, but based on the demonstrated modulatory effects of inflammation on the developing brain (exposure of a neonatal brain to low concentration of lipopolysaccharide[30]), it is conceivable that increased modest cytokine release, both locally and systemically, trigger caspase-3 activation when necrosis is minimal.

In summary, although the underlying mechanisms of ADC reduction are yet to be fully understood, these data provide the basis for using DWI at 24 hours postinjury as a surrogate measure for the presence of apoptotic-like cell death and caspase-3 activation in the neonate after H-I.

Acknowledgments

Sources of Funding

This study was funded by National Institutes of Health grants NS35902 (to D.M.H. and Z.S.V.) and NS44025 and American Heart Association 0655236Y (to Z.S.V.).

References

1. Inder TE, Huppi PS. In vivo studies of brain development by magnetic resonance techniques. Ment Retard Dev Disabil Res Rev. 2000; 6:59–67. [PubMed: 10899798]
2. Ferriero DM. Neonatal brain injury. N Engl J Med. 2004; 351:1985–1995. [PubMed: 15525724]
3. Dijkhuizen RM, van Lookeren Campagne M, Niendorf T, Dreher W, van der Toorn A, Hoehn-Berlage M, Verheul HB, Tulleken CA, Leibfritz D, Hossmann KA, Nicolay K. Status of the neonatal rat brain after NMDA-induced excitotoxic injury as measured by MRI, MRS and metabolic imaging. NMR Biomed. 1996; 9:84–92. [PubMed: 8887373]
4. Dijkhuizen RM, Knollema S, van der Worp HB, Ter Horst GJ, De Wildt DJ, Berkelbach van der Sprenkel JW, Tulleken KA, Nicolay K. Dynamics of cerebral tissue injury and perfusion after temporary hypoxia–ischemia in the rat: evidence for region-specific sensitivity and delayed damage. Stroke. 1998; 29:695–704. [PubMed: 9506615]
5. Tuor UI, Kozlowski P, Del Bigio MR, Ramjiawan B, Su S, Malisza K, Saunders JK. Diffusion- and T2-weighted increases in magnetic resonance images of immature brain during hypoxia–ischemia: transient reversal posthypoxia. Exp Neurol. 1998; 150:321–328. [PubMed: 9527902]
6. Derugin N, Wendland M, Muramatsu K, Roberts T, Gregory G, Ferriero D, Vexler Z. Evolution of brain injury after transient middle cerebral artery occlusion in neonatal rat. Stroke. 2000; 31:1752–1761. [PubMed: 10884483]
7. Manabat C, Han BH, Wendland M, Derugin N, Fox CK, Choi J, Holtzman DM, Ferriero DM, Vexler ZS. Reperfusion differentially induces caspase-3 activation in ischemic core and penumbra after stroke in immature brain. Stroke. 2003; 34:207–213. [PubMed: 12511776]
8. van Bruggen N, Cullen BM, King MD, Doran M, Williams SR, Gadian DG, Cremer JE. T2- and diffusion-weighted magnetic resonance imaging of a focal ischemic lesion in rat brain. Stroke. 1992; 23:576–582. [PubMed: 1373254]
9. Ashwal S, Tone B, Tian HR, Chong S, Obenaus A. Comparison of two neonatal ischemic injury models using magnetic resonance imaging. Pediatr Res. 2007; 61:9–14. [PubMed: 17211133]

10. Derugin N, Dingman A, Wendland M, Fox C, Vexler ZS. Magnetic resonance imaging as a surrogate measure for histological sub-chronic endpoint in a neonatal rat stroke model. Brain Res. 2005; 1066:49–56. [PubMed: 16336947]
11. Wang Y, Cheung PT, Shen GX, Wu EX, Cao G, Bart I, Wong WH, Khong PL. Hypoxic–ischemic brain injury in the neonatal rat model: Relationship between lesion size at early MR imaging and irreversible infarction. AJNR Am J Neuroradiol. 2006; 27:51–54. [PubMed: 16418355]
12. Rumpel H, Nedelcu J, Aguzzi A, Martin E. Late glial swelling after acute cerebral hypoxia–ischemia in the neonatal rat: a combined magnetic resonance and histochemical study. Pediatr Res. 1997; 42:54–59. [PubMed: 9212037]
13. Qiao M, Malisza KL, Del Bigio MR, Tuor UI. Transient hypoxia–ischemia in rats: changes in diffusion-sensitive MR imaging findings, extracellular space, and Na+-K+-adenosine triphosphatase and cytochrome oxidase activity. Radiology. 2002; 223:65–75. [PubMed: 11930049]
14. Cheng Y, Gidday JM, Yan Q, Shah AR, Holtzman DM. Marked age-dependent neuroprotection by brain-derived neurotrophic factor against neonatal hypoxic–ischemic brain injury. Ann Neurol. 1997; 41:521–529. [PubMed: 9124810]
15. Hu BR, Liu CL, Ouyang Y, Blomgren K, Siesjo BK. Involvement of caspase-3 in cell death after hypoxia–ischemia declines during brain maturation. J Cereb Blood Flow Metab. 2000; 20:1294–1300. [PubMed: 10994850]
16. Han BH, Holtzman DM. BDNF protects the neonatal brain from hypoxic–ischemic injury in vivo via the ERK pathway. J Neurosci. 2000; 20:5775–5781. [PubMed: 10908618]
17. Han BH, Xu D, Choi J, Han Y, Xanthoudakis S, Roy S, Tam J, Vaillancourt J, Colucci J, Siman R, Giroux A, Robertson GS, Zamboni R, Nicholson DW, Holtzman DM. Selective, reversible caspase-3 inhibitor is neuroprotective and reveals distinct pathways of cell death following neonatal hypoxic–ischemic brain injury. J Biol Chem. 2002; 277:30128–30136. [PubMed: 12058036]
18. Fox C, Dingman A, Derugin N, Wendland MF, Manabat C, Ji S, Ferriero DM, Vexler ZS. Minocycline confers early but transient protection in the immature brain following focal cerebral ischemia–reperfusion. J Cereb Blood Flow Metab. 2005; 25:1138–1149. [PubMed: 15874975]
19. Dingman A, Lee SY, Derugin N, Wendland MF, Vexler ZS. Amino-guanidine inhibits caspase-3 and calpain activation without affecting microglial activation following neonatal transient ischemia. J Neurochem. 2006; 96:1467–1479. [PubMed: 16464234]
20. Blomgren K. Calpastatin is upregulated and acts as a suicide substrate to calpains in neonatal rat hypoxia–ischemia. Ann N Y Acad Sci. 1999; 890:270–271. [PubMed: 10668432]
21. Han BH, DeMattos RB, Dugan LL, Kim-Han JS, Brendza RP, Fryer JD, Kierson M, Cirrito J, Quick K, Harmony JA, Aronow BJ, Holtzman DM. Clusterin contributes to caspase-3-independent brain injury following neonatal hypoxia–ischemia. Nat Med. 2001; 7:338–343. [PubMed: 11231633]
22. Matsumori Y, Northington F, Hong SM, Kayama T, Sheldon RA, Vexler ZS, Ferriero DM, Weinstein PR, Liu J. Reduction of caspase-9 cleavage is associated with increased binding of APAF-1 and HSP70 after neonatal hypoxic/ischemic injury in mice over-expressing HSP70. Stroke. 2006; 37:507–512. [PubMed: 16397188]
23. Cheng Y, Deshmukh M, D'Costa A, Demaro JA, Gidday JM, Shah A, Sun Y, Jacquin MF, Johnson EM, Holtzman DM. Caspase inhibitor affords neuroprotection with delayed administration in a rat model of neonatal hypoxic–ischemic brain injury. J Clin Invest. 1998; 101:1992–1999. [PubMed: 9576764]
24. Dijkhuizen RM, de Graaf RA, Tulleken KA, Nicolay K. Changes in the diffusion of water and intracellular metabolites after excitotoxic injury and global ischemia in neonatal rat brain. J Cereb Blood Flow Metab. 1999; 19:341–349. [PubMed: 10078886]
25. Ashwal S, Tone B, Tian HR, Chong S, Obenaus A. Serial magnetic resonance imaging in a rat pup filament stroke model. Exp Neurol. 2006; 202:294–301. [PubMed: 16876160]
26. Ringer TM, Neumann-Haefelin T, Sobel RA, Moseley ME, Yenari MA. Reversal of early diffusion-weighted magnetic resonance imaging abnormalities does not necessarily reflect tissue salvage in experimental cerebral ischemia. Stroke. 2001; 32:2362–2369. [PubMed: 11588327]

27. Hedtjarn M, Mallard C, Hagberg H. Inflammatory gene profiling in the developing mouse brain after hypoxia–ischemia. J Cereb Blood Flow Metab. 2004; 24:1333–1351. [PubMed: 15625408]
28. Siesjo BK. Pathophysiology and treatment of focal cerebral ischemia. Part I: pathophysiology. J Neurosurg. 1992; 77:169–184. [PubMed: 1625004]
29. Northington FJ, Graham EM, Martin LJ. Apoptosis in perinatal hypoxic–ischemic brain injury: how important is it and should it be inhibited? Brain Res Brain Res Rev. 2005; 50:244–257. [PubMed: 16216332]
30. Hagberg H, Mallard C. Effect of inflammation on central nervous system development and vulnerability. Curr Opin Neurol. 2005; 18:117–123. [PubMed: 15791140]

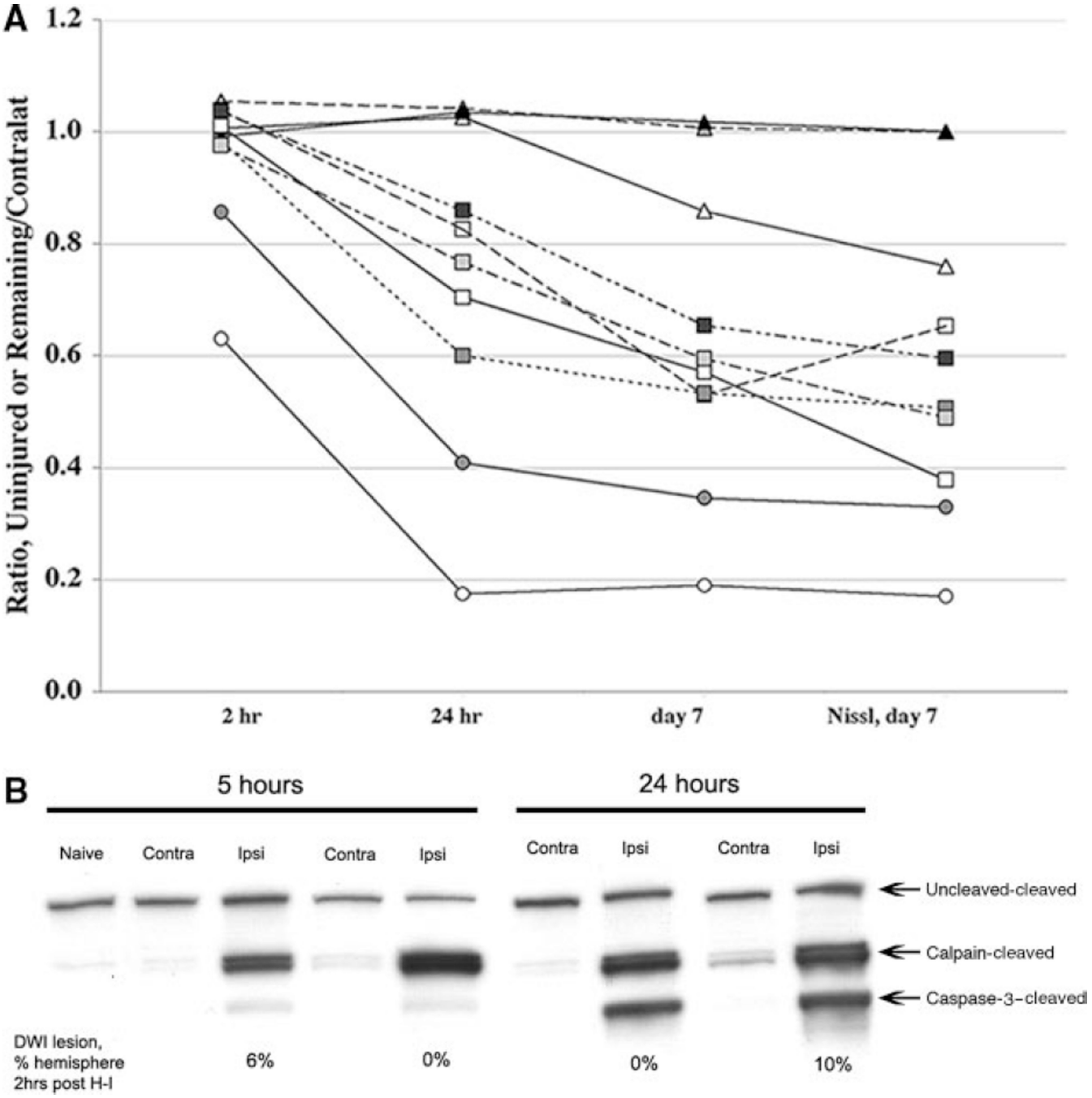

Figure 1.

A, Injury evolution identified by MRI and corresponding histology. MRI was performed at 2 hours, 24 hours, and 7 days after H-I in 10 pups. For the 2- and 24-hour time points, the extent of injury on DWI maps is expressed as the difference between the volume of noninjured ipsilateral hemisphere divided by the volume of the contralateral hemisphere. For the 7-day time point, measurements are done on T2-weighted images and are expressed as the remaining tissue in ipsilateral hemisphere divided by the tissue in the contralateral hemisphere. B, DWI shortly after H-I does not predict the calpain or caspase-3 activation.

Calpain activation occurs 5 hours after H-I in animals with no or small (6% of ipsilateral hemisphere) DWI lesions 2 hours after H-I. Both calpain- and caspase-3-dependent spectrin cleavage are seen 24 hours after H-I in animals with no early DWI lesions. Contra, contralateral; ipsi, ipsilateral.

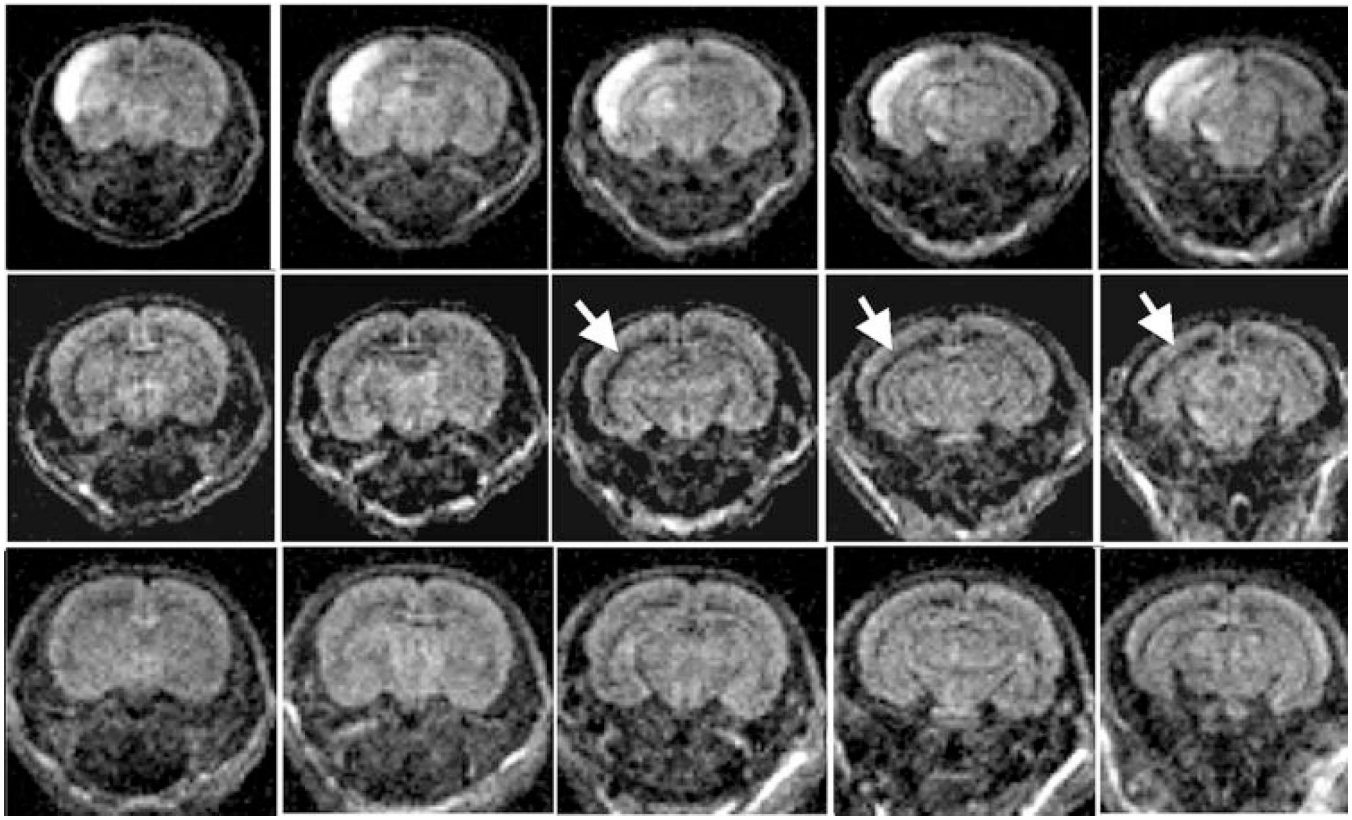

Figure 2.

Examples of 3 levels of DWI injury at 24 hours after H-I. Diffusion hyperintensity of ipsilateral cortex with additional patchy hyperintensity in subcortical regions (group 1, top). Enlargement of lateral ventricle (group 2, middle). No injury (group 3, bottom).

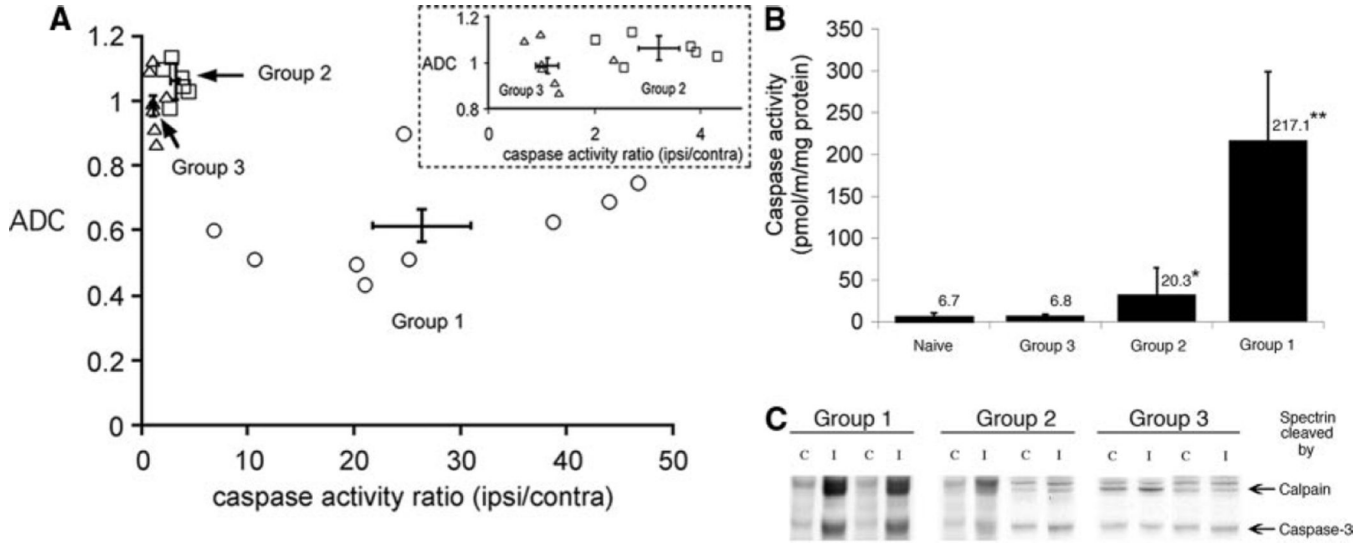

Figure 3.

DWI lesions and caspase-3 activation 24 hours post-H-I. A, ADC of ipsilateral cortical region versus normalized caspase-3 activity (activity in ipsilateral cortex/contralateral cortex). All animals with markedly elevated caspase-3 activity had a reduced ADC value in the ipsilateral cortex. Error bar crosshair shows mean±SD in group 1. Inset, Expanded region for groups 2 and 3. Note that ADC of the cortical tissue was the same for both subgroups, whereas the caspase-3 activity ratio was significantly greater in group 2. B, Caspase-3 activity in brain homogenates from animals in groups 1 to 3. Mean±SD; n=6 to 9 per group. *P<0.05; **P<0.01 in comparison to uninjured. C, In animals imaged 24 hours after H-I, a substantial caspase-3-dependent spectrin cleavage occur in group 1, whereas subtle to no cleavage is seen in groups 2 and 3, respectively. C, contralateral; I, ipsilateral.

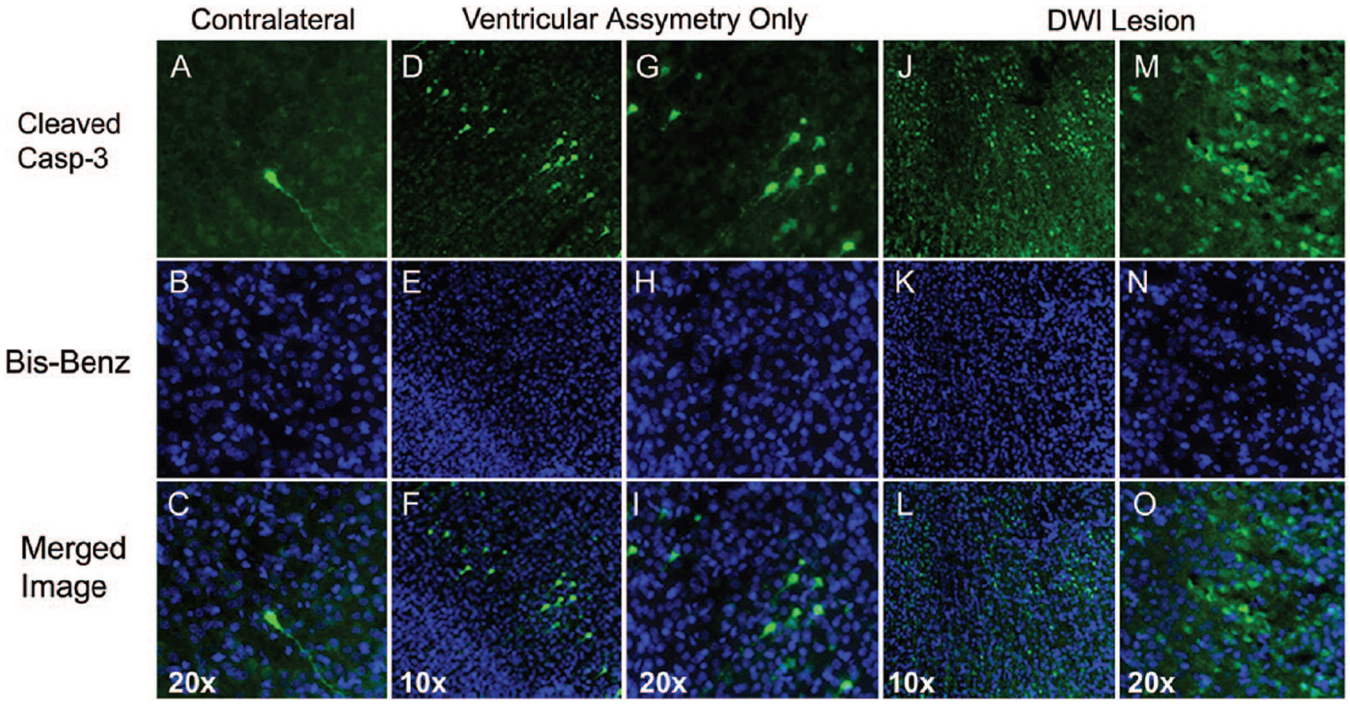

Figure 4.

Localization of cleaved caspase-3 24 hours post-H-I. A–C, Only occasional cells with cleaved caspase-3 are seen in hypoxic hemisphere in each brain studied. Cleaved caspase-3 is present in both cell body and processes of the shown cell (A, C, green). D–I, Scattered cells with cleaved caspase-3 are present in the cortex of pups in group 2. Many cells are in early apoptotic stages as seen from cell morphology (D and G) and the appearance of the nuclei (E and H). J–O, Marked number of cells with cleaved caspase-3 is seen ipsilateral in animals in group 1. C, F, I, L, and O, Overlay of cleaved caspase-3(green)/bis-benzamide (blue).

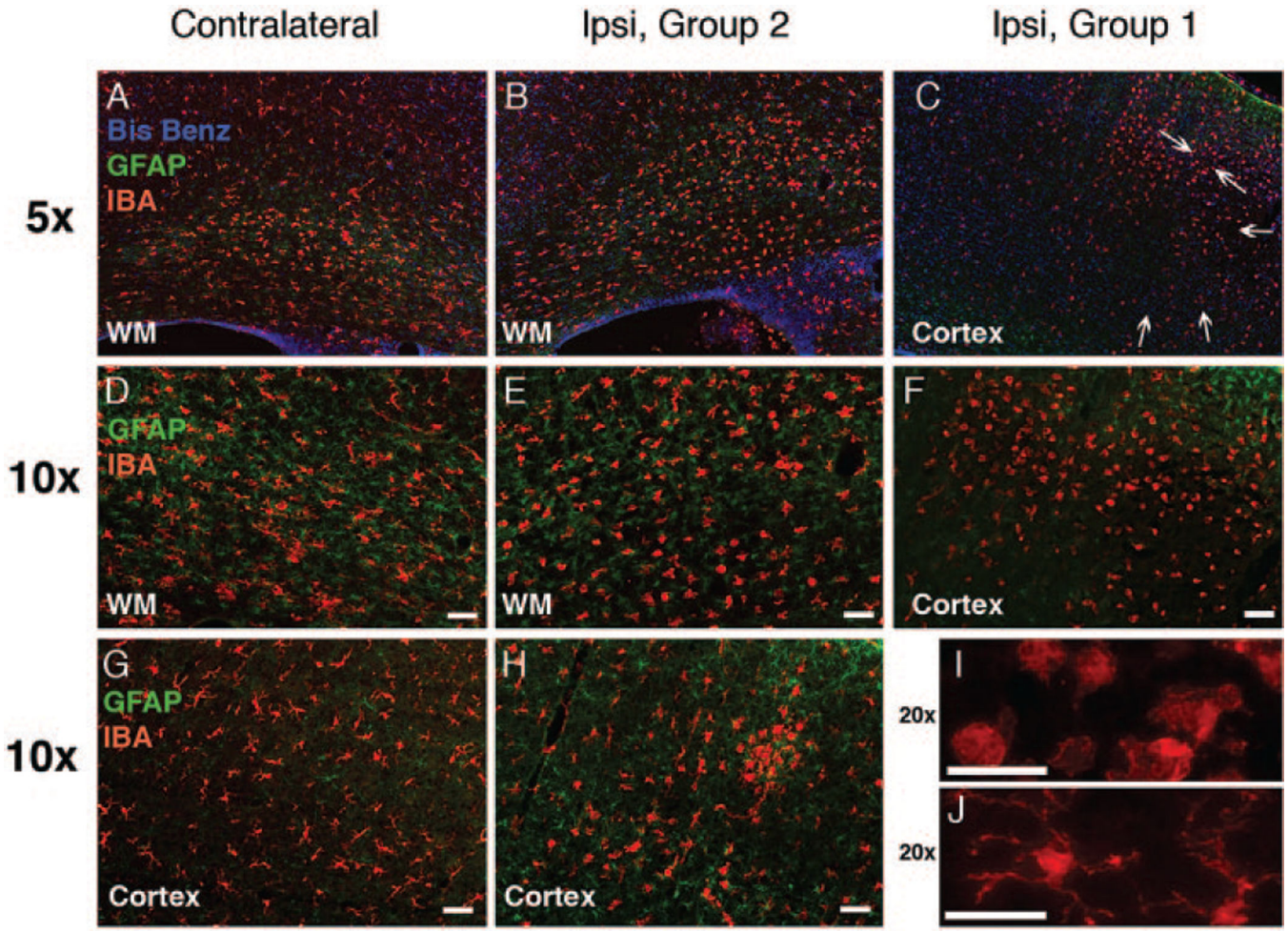

Figure 5.

Microglial activation and reactive astrogliosis associated with profound and modest caspase-3 activation 24 hours after H-I. A–J, Compared with the contralateral hemisphere (A, D, G), a range of microglial morphologies (Iba1, red) is seen in the hemisphere ipsilateral to modest H-I injury (group 2, B, E, H). Accumulation of activated Iba1-positive cells is seen in group 1 (C, F, I). Note a major difference in morphological transformation of microglial cells in group 2 compared with group 1. I–J, Higher magnification picture (20× objective) of activated (I) and resting (J) microglia. Arrows in C indicate substantial damage (morphology of Bis-Benzamide). Modest reactive astrocytosis in the white matter of the H-I hemisphere, group 2 (B, E, glial fibrillary acidic protein, green). In group 1, reactive astrogliosis occurs predominantly outside of severely injured regions (C, F).